pISSN 2384-1095
eISSN 2384-1109

iMRI 2018;22:229-239

https://doi.org/10.13104/imri.2018.22.4.229

iMRI
Investigative Magnetic Resonance Imaging

Diagnosis of Rotator Cuff Tears with Non-Arthrographic MR Imaging: 3D Fat-Suppressed Isotropic Intermediate-Weighted Turbo Spin-Echo Sequence versus Conventional 2D Sequences at 3T

Won Sun Hong[1,2], Won-Hee Jee[1], So-Yeon Lee[1,3], Chang-Woo Chun[1,4], Joon-Yong Jung[1], Yang-Soo Kim[5]

[1]Department of Radiology, Seoul St. Mary's Hospital, School of Medicine, The Catholic University of Korea, Seoul, Korea
[2]Department of Radiology, Seoul Bumin Hospital, Seoul, Korea
[3]Department of Radiology, Kangbuk Samsung Hospital, Sungkyunkwan University School of Medicine, Seoul, Korea
[4]Department of Radiology, Uijongbu St. Mary's Hospital, School of Medicine, The Catholic University of Korea, Gyeonggi-do, Korea
[5]Department of Orthopedic Surgery, Seoul St. Mary's Hospital, School of Medicine, The Catholic University of Korea, Seoul, Korea

Original Article

Received: September 11, 2018
Revised: November 3, 2018
Accepted: November 16, 2018

Correspondence to:
Won-Hee Jee, M.D.
Department of Radiology, Seoul St. Mary's Hospital, School of Medicine, The Catholic University of Korea, 222 Banpo-daero, Seocho-gu, Seoul 06591, Korea.
Tel. +82-2-2258-6238
Fax. +82-2-599-6771
E-mail: whjee12@gmail.com

Purpose: To assess the diagnostic performance in detecting rotator cuff tears at 3T of non-arthrographic shoulder magnetic resonance imaging (MRI) using 3D isotropic turbo spin-echo (TSE-SPACE) sequence as compared with 2D sequences.

Materials and Methods: Seventy-four patients who were arthroscopically confirmed to have underwent non-arthrographic shoulder MRI with 2D sequences and TSE-SPACE were included. Three independent readers retrospectively scored supraspinatus and infraspinatus tendon (SST-IST) and subscapularis tendon (SCT) tears on 2D sequences and TSE-SPACE.

Results: The mean sensitivity, specificity, and accuracy of the three readers were 95%, 100%, and 95% on TSE-SPACE and 99%, 93%, and 98% on 2D sequences for detecting SST-IST tears, respectively, whereas those were 87%, 49%, and 68% on TSE-SPACE and 88%, 66%, and 77% on 2D sequences for detecting SCT tears, respectively. There was no statistical difference between the two sequences, except for in the specificity of one reader for detecting SCT tears. The mean AUCs of the three readers on TSE-SPACE and 2D sequences were 0.96 and 0.98 for detecting SST-IST tears, respectively, which were not significantly different, while those were 0.71 and 0.82 for detecting SCT tears, respectively, which were significantly different ($P < 0.05$).

Conclusion: TSE-SPACE may have accuracy and reliability comparable to conventional 2D sequences for SST-IST tears at non-arthrographic 3T shoulder MRI, whereas TSE-SPACE was less reliable than conventional 2D sequences for detecting SCT tears.

Keywords: Rotator cuff; Magnetic resonance imaging; Non-arthrographic; 3D isotropic; SPACE

INTRODUCTION

Magnetic resonance (MR) arthrography has been reported to be the most sensitive and specific method for assessing rotator cuff tears (1). However, the majority of these reports were based on studies performed at intermediate field strengths of 1.5T or lower. Recently, 3T MR imaging (MRI) has become increasingly available for clinical use, and the increased signal-to-noise ratio in 3T MRI offers superior imaging resolution and shortened imaging time (2, 3). With the widespread use of 3T MRI, questions have arisen as to whether MR arthrography is necessary for diagnosing rotator cuff tears at 3T. Moreover, direct MR arthrography necessarily brings an issue related to the coordination of scheduling in two procedure rooms, as well as intraarticular needle placement, which is mildly invasive and can cause pain and discomfort (4).

In recent years, the three-dimensional (3D) isotropic fast spin-echo (FSE) sequence has been spotlighted due to the thin continuous sections and feasibility of multiplanar reformation (5-10). Previous studies (5-17) have assessed the diagnostic performance of 3D isotropic FSE sequence in various joints at 3T. Among them, several studies (5-7, 9-11) have found the diagnostic performance of shoulder MR arthrography with a FSE-based 3D isotropic sequence to be comparable to that of conventional two-dimensional (2D) sequences. However, the diagnostic performance of non-arthrographic shoulder MRI using 3D isotropic FSE sequence has rarely been reported. Thus, we evaluated the diagnostic performance of non-arthrographic shoulder MRI using 3D isotropic turbo spin-echo (TSE-SPACE) sequence as compared with conventional 2D TSE sequences for detecting rotator cuff tears at 3T.

MATERIALS AND METHODS

Subjects

The study was approved by our Institutional Review Board, and informed consent was waived for this retrospective study. Between March 2012 and November 2012, 404 patients underwent non-arthrographic shoulder 3T MRI at our institution. Seven patients were excluded due to infection (n = 1), avascular necrosis (n = 2), diffuse tenosynovial giant cell tumor (n = 1), and the lack of available TSE-SPACE images (n = 3). Among them, 83 underwent shoulder arthroscopic surgery, of which two were excluded because the interval between MRI and arthroscopic surgery was longer than five months. In addition, seven patients were excluded due to insufficient sequences (n = 6) and large joint effusion mimicking the effect of direct arthrography (n = 1). As a result, 74 patients (35 men and 39 women; age range, 38-84 years; mean age, 62 years) were ultimately included in this study (Fig. 1).

MR Imaging

All MR images were obtained using a 3T MR unit (Magnetom Verio; Siemens Healthcare, Erlangen, Germany) with an eight-channel phased-array shoulder coil. All patients were scanned in the supine position with their arms in neutral position. Conventional 2D imaging was performed first, followed by 3D fat-suppressed (FS) isotropic intermediate-weighted TSE-SPACE. FS T2-weighted images were obtained in the axial, coronal oblique, and sagittal oblique planes. T2-weighted images were obtained in the coronal oblique and sagittal oblique planes. FS proton density (PD) images were obtained in a coronal oblique plane. We performed the TSE-SPACE in a coronal oblique plane, and the source data were reformatted into axial and sagittal oblique planes with 0.6 mm slice thickness and no interslice gap. Postprocessing was performed by

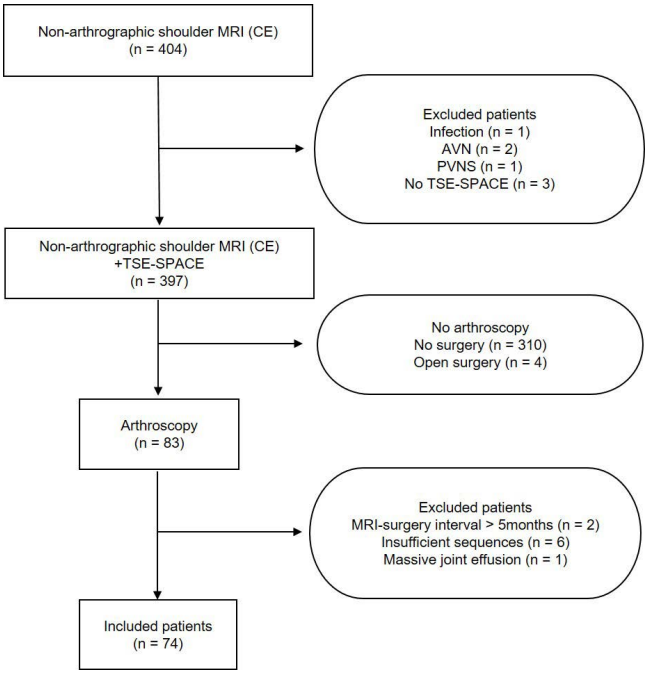

Fig. 1. Flow diagram of the study. AVN = avascular necrosis; CE = contrast-enhancement; GCT = giant cell tumor; PVNS = pigmented villonodular synovitis; TSE-SPACE = three-dimensional isotropic fat-suppressed turbo spin-echo SPACE intermediate-weighted image

technologists with the use of commercially available software (Syngo MR, Siemens). The imaging parameters of each sequence are summarized in Table 1.

Image Analysis

MR images were retrospectively analyzed by three independent readers who were blind to the arthroscopy results and clinical information: three musculoskeletal radiologists (BLIND, BLIND, BLIND with 16, five, and two years of experience in musculoskeletal radiology, respectively). They evaluated the MR images to detect supraspinatus tendon (SST)-infraspinatus tendon (IST) tears and subscapularis tendon (SCT) tears. The following imaging criteria were integrated for the determination of the rotator cuff tendons as normal or abnormal: change of tendon morphology, discontinuity of the tendon, focal signal alteration of the tendon, and caliber changes. The presence of tears in the rotator cuff was scored using a five-point confidence scale during each session of the analyses: 0, definitely absent; 1, probably absent; 2, equivocal; 3, probably present; 4, definitely present. Scores of 0-2 were considered negative and scores of 3-4 were considered positive. When SST-IST and SCT tears were scored as 3 or 4, the tears were classified as either full- or partial-thickness tears. Partial-thickness tears were categorized further as either articular or bursal surface tears. An intratendinous tear was diagnosed in cases where there was an intratendinous high signal that did not extend either to the articular or bursal surface.

For the first step, TSE-SPACE was analyzed in a randomized order. After three weeks, conventional 2D images were analyzed in a randomized order for the second step. Upon completion of the two steps, the misinterpreted cases were re-reviewed in consensus between three readers. Arthroscopic findings were used as the reference standard. Arthroscopy was performed by an orthopedic surgeon (BLIND) with 14 years of experience. In order to improve the visualization of SCT footprint, an anterior portal was made slightly lateral to the coracoid tip through the rotator interval besides the standard portal. The assistant should push the patient's shoulder backward so as to obtain wide subacromial space. The mean interval between the MRI and arthroscopy was 63 days (range, eight-146 days).

Statistics

The sensitivities, specificities, and accuracies of the three readers were calculated in order to compare the diagnostic performances between 2D sequences and TSE-SPACE in the diagnosis of SST-IST and SCT tears. McNemar's test was used to compare 2D sequences and TSE-SPACE. In addition, sensitivity, specificity, and accuracy were calculated again for each reader and for each sequence of 2D sequences. The interobserver agreements between three readers for 2D sequences and TSE-SPACE were calculated using κ coefficients. The κ values were interpreted as follows: < 0.20, poor; 0.21-0.40, fair; 0.41-0.60, moderate; 0.61-0.80, substantial; 0.81-1.00, very good (18). In order to evaluate the overall performance of the readers, the data were analyzed through the receiver operative characteristic (ROC) method. Statistical significance was assumed for

Table 1. MR Imaging Parameters

Parameter	3D TSE-SPACE	Conventional 2D sequences					
		Axial FS T2WI	Coronal FS T2WI	Sagittal FS T2WI	Coronal T2WI	Sagittal T2WI	Coronal FS PDI
Repetition time (ms)	1000	5720	4640	4800	4200	4510	3000
Echo time (ms)	55	57	58	57	58	58	27
Matrix size	192 × 192	512 × 256	512 × 256	512 × 256	512 × 256	512 × 256	448 × 224
Field of view (cm)	140 × 140	140 × 140	140 × 140	140 × 140	140 × 140	140 × 140	140 × 140
Section thickness (mm)	0.6	3	2.5	3	2.5	3	2.5
Intersection gap (mm)	0	0	0	0	0	0	0
Echo train length	127	13	13	13	13	13	4
Bandwidth (Hz/pixel)	457	127	120	120	250	250	120
Imaging time	8 min 24 sec	2 min 34 sec	4 min 48 sec	3 min 58 sec	2 min 55 sec	3 min 14 sec	4 min 11 sec

2D = two-dimensional; 3D TSE-SPACE = three-dimensional isotropic fat-suppressed turbo spin-echo SPACE intermediate-weighted image; FS = fat-suppressed; PD = proton density; T2WI = T2-weighted images

P < 0.05. All statistical analyses were performed using the commercial software (SPSS, version 19, SPSS, IBM, Armonk, New York and MedCalc Software, version 11.3.0.0, Mariakerke, Belgium).

RESULTS

The sensitivities and specificities with corresponding 95% confidence intervals, as well as the accuracies of 2D sequences and TSE-SPACE for the diagnosis of rotator cuff tears by three readers are summarized in Table 2. The AUCs showing the diagnostic performance of three readers in the detection of rotator cuff tears are summarized in Table 3. The interobserver agreements of three readers in evaluating rotator cuff tears are shown in Table 4.

SST-IST Tears

Arthroscopy revealed 35 full-thickness tears and 34 partial-thickness tears (27 bursal-sided tears, seven articular-sided tears) of the SST-IST (Figs. 2, 3a, b). The mean sensitivities, specificities, and accuracies of the three readers were 95%, 100%, and 95% on TSE-SPACE and 99%, 93%, 98% on 2D sequences for detecting all (full-thickness and partial-thickness) SST-IST tears. For detecting partial-thickness SST-IST tears, the mean sensitivity, specificity, and accuracy of the three readers were 91%, 98%, and 95% on TSE-SPACE and 97%, 99%, and 98% on 2D sequences,

Table 2. Diagnostic Performance of Conventional 2D Sequences and 3D TSE-SPACE in Evaluating Rotator Cuff Tears

		Sensitivity			Specificity			Accuracy	
		3D TSE-SPACE	2D TSE	P-value	3D TSE-SPACE	2D TSE	P-value	3D TSE-SPACE	2D TSE
SST-IST tear									
FT+PT	Reader1	93 (64/69) [84, 97]	99 (68/69) [92, 100]	0.125	100 (5/5) [57, 100]	100 (5/5) [57, 100]	NA	93 (69/74)	99 (73/74)
	Reader2	96 (66/69) [88, 99]	99 (68/69) [92, 100]	0.500	100 (5/5) [57, 100]	80 (4/5) [38, 96]	NA	96 (71/74)	97 (72/74)
	Reader3	96 (66/69) [88, 99]	99 (68/69) [92, 100]	0.500	100 (5/5) [57, 100]	100 (5/5) [57, 100]	NA	96 (71/74)	99 (73/74)
PT	Reader1	91 (31/34) [77, 97]	97 (33/34) [85, 100]	0.500	95 (38/40) [84, 99]	100 (40/40) [91, 100]	0.500	93 (69/74)	99 (73/74)
	Reader2	91 (31/34) [77, 97]	97 (33/34) [85, 100]	0.500	100 (40/40) [91, 100]	98 (39/40) [87, 100]	1.000	96 (71/74)	97 (72/74)
	Reader3	91 (31/34) [77, 97]	97 (33/34) [85, 100]	0.500	100 (40/40) [91, 100]	100 (40/40) [91, 100]	1.000	96 (71/74)	99 (73/74)
FT	Reader1	94 (33/35) [81, 98]	100 (35/35) [90,100]	0.500	100 (39/39) [91, 100]	100 (39/39) [91, 100]	NA	97 (72/74)	100 (74/74)
	Reader2	100 (35/35) [90, 100]	100 (35/35) [90, 100]	NA	100 (39/39) [91, 100]	100 (39/39) [91, 100]	NA	100 (74/74)	100 (74/74)
	Reader3	100 (35/35) [90, 100]	100 (35/35) [90, 100]	NA	100 (39/39) [91, 100]	100 (39/39) [91, 100]	NA	100 (74/74)	100 (74/74)
SCT tear									
	Reader1	92 (35/38) [79, 97]	87 (33/38) [73, 94]	0.687	31 (11/36) [18, 47]	61 (22/36) [45, 75]	0.001	62 (46/74)	74 (55/74)
	Reader2	82 (31/38) [67, 91]	87 (33/38) [73, 94]	0.625	50 (18/36) [35, 66]	61 (22/36) [45, 75]	0.219	66 (49/74)	74 (55/74)
	Reader3	87 (33/38) [73, 94]	90 (34/38) [76, 96]	0.000	67 (24/36) [50, 80]	75 (27/36) [59, 86]	0.375	77 (57/74)	82 (61/74)

Data in parentheses are numbers of lesions. Data in square brackets are 95% confidence interval.
2D = two-dimensional; 3D TSE-SPACE = three-dimensional isotropic fat-suppressed turbo spin-echo SPACE intermediate-weighted image; FT = full-thickness tear; NA = non-applicable; PT = partial-thickness tear; SCT = subscapularis tendon; SST-IST = supraspinatus and infraspinatus tendon

Table 3. Area Under Receiver Operating Characteristics Curve (AUC) of Three Readers in Evaluating Rotator Cuff Tears

		Reader 1	Reader 2	Reader 3	Reader 1-2 P-value	Reader 1-3 P-value	Reader 2-3 P-value
SST-IST tear							
FT+PT	3D TSE-SPACE	0.964 ± 0.0197	0.959 ± 0.0233	0.957 ± 0.0247	0.863 (-0.045, 0.054)	0.763 (-0.040, 0.054)	0.920 (-0.053, 0.059)
	2D TSE	0.991 ± 0.0088	0.975 ± 0.0253	0.987 ± 0.0131	0.544 (-0.036, 0.067)	0.784 (-0.027, 0.036).	0.675 (-0.043, 0.066)
	P-value	0.105 (-0.006, 0.061)	0.612 (-0.047, 0.079)	0.136 (-0.010, 0.071)			
PT	3D TSE-SPACE	0.944 ± 0.0353	0.918 ± 0.0465	0.912 ± 0.0494	0.583 (-0.068, 0.121)	0.472 (-0.056, 0.120)	0.920 (-0.109, 0.121)
	2D TSE	0.982 ± 0.0179	0.953 ± 0.0480	0.974 ± 0.0266	0.559 (-0.069, 0.128)	0.786 (-0.055, 0.072)	0.700 (-0.084, 0.125)
	P-value	0.178 (-0.017, 0.094)	0.572 (-0.087, 0.158)	0.132 (-0.019, 0.142)			
SCT tear							
	3D TSE-SPACE	0.641 ± 0.0581	0.682 ± 0.0538	0.791 ± 0.0495	0.454 (-0.066, 0.147)	0.007 (0.042, 0.258)	0.012 (0.024, 0.194)
	2D TSE	0.798 ± 0.0499	0.794 ± 0.0495	0.865 ± 0.0416	0.910 (-0.066, 0.074)	0.061 (-0.003, 0.136)	0.065 (-0.004, 0.145)
	P-value	0.005 (0.047, 0.268)	0.010 (0.026, 0.199)	0.035 (0.005, 0.143)			

Data are AUC values ± standard errors. Data in parentheses are 95% confidence interval.
2D = two-dimensional; 3D TSE-SPACE = three-dimensional isotropic fat-suppressed turbo spin-echo SPACE intermediate-weighted image; FT = full-thickness tear; NA = non-applicable; PT = partial-thickness tear; SCT = subscapularis tendon; SST-IST = supraspinatus and infraspinatus tendon

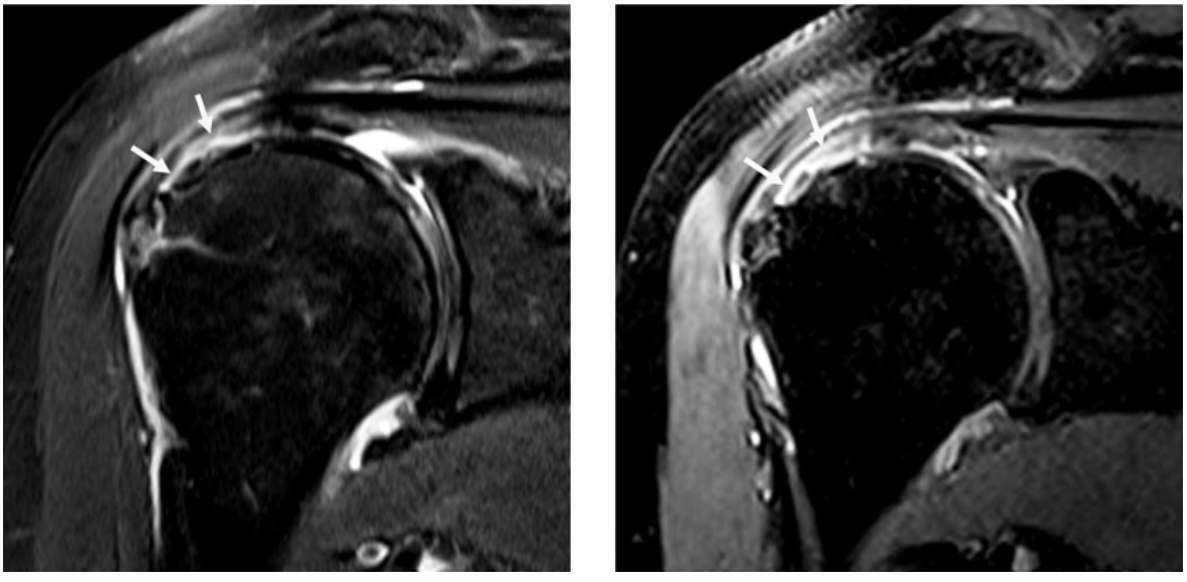

a b

Fig. 2. Non-arthrographic MR images show arthroscopically-proven partial-thickness articular-sided tear of the SST-IST in a 68-year-old woman. (a) Oblique coronal fat-suppressed T2-weighted image and (b) 3D isotropic fat-suppressed intermediate-weighted TSE-SPACE image show a partial-thickness articular-sided tear (arrows) of the SST-IST. All three readers correctly interpreted this case on both 2D sequences and TSE-SPACE.

respectively. There were no significant differences in sensitivity, specificity, or accuracy between TSE-SPACE and 2D sequences for either readers in all SST-IST tears or in partial-thickness SST-IST tears alone. The areas under the curve (AUCs) of reader 1, 2, and 3 using TSE-SPACE versus those of reader 1, 2, and 3 using 2D sequences for all SST-

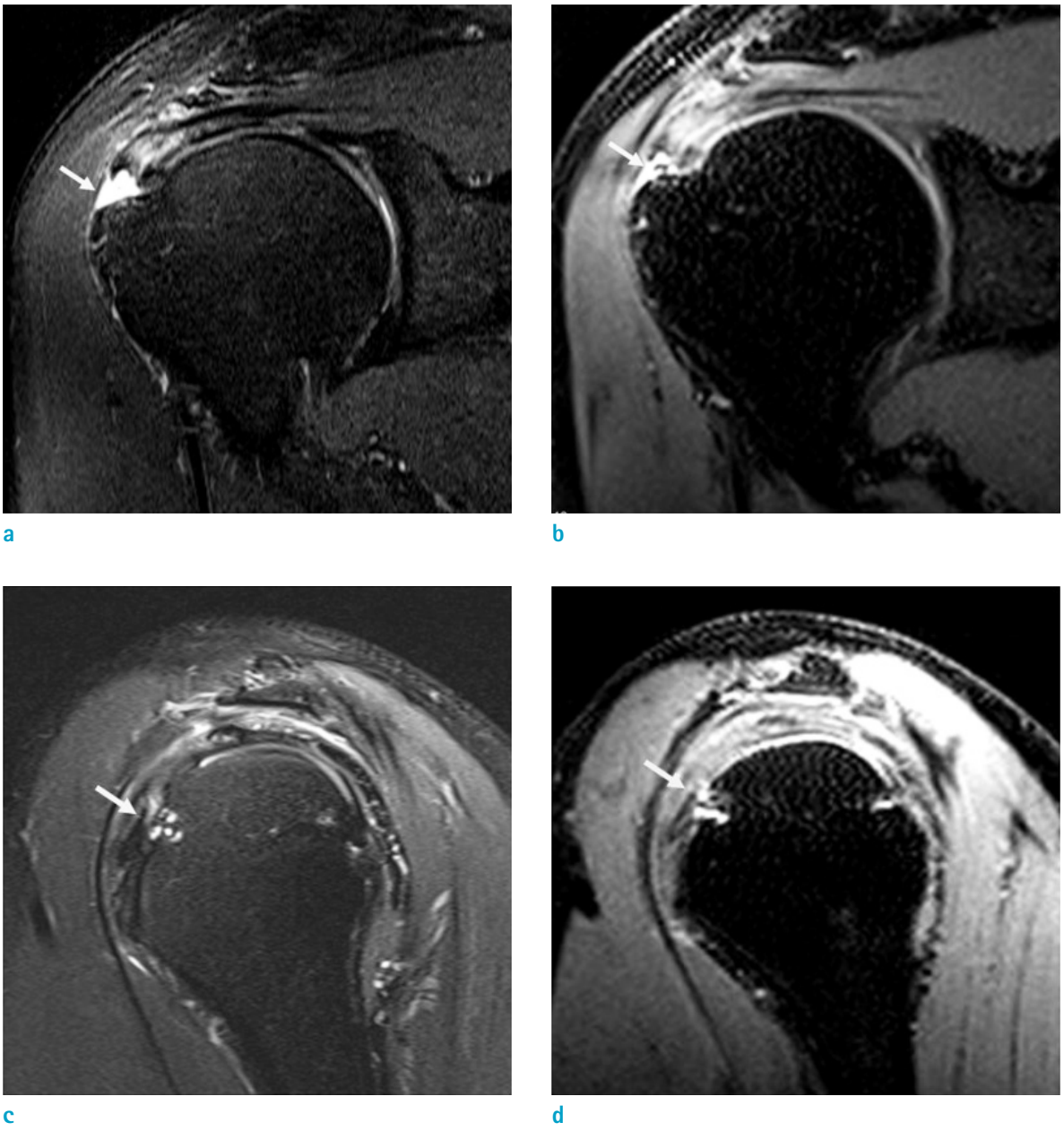

Fig. 3. Non-arthrographic MR images show arthroscopically-proven partial-thickness bursal-sided tear of SST-IST and intact SCT in a 55-year-old man. (a) Oblique coronal fat-suppressed T2-weighted image and (b) 3D isotropic fat-suppressed intermediate-weighted TSE-SPACE image show a partial-thickness bursal-sided tear (arrows) of the SST-IST. (c) Oblique sagittal fat-suppressed T2-weighted image and (d) 3D isotropic fat-suppressed intermediate-weighted TSE-SPACE image with an oblique sagittal reformatted image show a subtle high signal intensity focus at the articular surface of SCT, which involves the superior portion of the tendon (arrows). A subcortical cyst is noted in the lesser tuberosity of proximal humerus. All three readers correctly interpreted the SST-IST on both 2D sequences and TSE-SPACE. However, they misinterpreted the SCT on both 2D sequences and TSE-SPACE.

IST tears were 0.964, 0.959, and 0.957 versus 0.991, 0.975, and 0.987, respectively. On 2D sequences, interobserver agreement was very good (κ = 0.90 and 0.82, respectively) between readers 1 and 2 as well as readers 1 and 3, and was substantial (κ = 0.71) between readers 2 and 3. On TSE-SPACE, interobserver agreement was substantial (κ = 0.75, 0.72, and 0.62, respectively) between readers 1 and 3, readers 2 and 3, and readers 1 and 2.

There were two false negative cases on 2D sequences and seven on TSE-SPACE in any of the three readers. Each reader missed one SST-IST tear with 2D sequences, with readers 1 and 2 missing the same case. The missed cases with 2D sequences were missed with TSE-SPACE. The two false negative cases on both 2D sequences and TSE-SPACE were retrospectively identifiable on re-review. One case was a superficial bursal-sided tear involving the anterior-most portion of the SST. The other case was a slit-like bursal-sided tear involving the junction of SST and IST. The remaining five cases, which were missed only on TSE-SPACE, were also all retrospectively identifiable on re-review. Two of five cases were non-retracted full-thickness tears on arthroscopy, which were presented as thin funnel-like cleft continuously seen on re-review in several planes traversing the tendon. The other three cases were partial-thickness bursal-sided tears. After correlation with the arthroscopic findings, the focal irregularity at the bursal surface of SST without definite discontinuity might be related to tendon degeneration or fraying.

SCT Tears

Arthroscopy revealed 35 partial-thickness tears and three full-thickness tears of SCT (Fig. 4). Regarding the detection of SCT tears, the mean sensitivity, specificity, and accuracy were 87%, 49%, and 68% on TSE-SPACE and 88%, 66%, and 77% on 2D sequences, respectively. There was no statistical difference between 2D sequences and TSE-SPACE, except for in specificity in one reader. The AUCs of readers 1, 2, and 3 using TSE-SPACE versus those of readers 1, 2, and 3 using 2D sequences were 0.641, 0.682, and 0.791 versus 0.798, 0.794, and 0.865, respectively. There was a statistically significant difference between 2D sequences and TSE-SPACE in each reader. On 2D sequences, interobserver agreement was substantial (κ = 0.71, 0.66, and 0.66, respectively) between readers 1 and 2, readers 2 and 3, and readers 1 and 3. Interobserver agreement was substantial (κ = 0.65) between readers 2 and 3 and fair (κ = 0.36 and 0.34, respectively) between readers 1 and 2 and readers 1 and 3 on TSE-SPACE.

There were 13 false negative cases in any of the three readers. Among them, three were only missed on 2D sequences and three were only missed on TSE-SPACE. Seven cases were missed on both 2D sequences and TSE-SPACE. One case was a false negative on both 2D sequences and TSE-SPACE in all three readers. This case was still equivocal on the second re-review. The remaining twelve cases were subtle but identifiable on the second re-review. There were 27 false positive cases in any of the three readers. Among them, 16 occurred on both 2D sequences and TSE-SPACE and 11 occurred only on TSE-SPACE. Seven cases were false positive on both 2D sequences and TSE-SPACE in all three readers (Fig. 3c, d). These cases were still thought to be positive for partial-thickness tears of SCT on the second re-review. After considering the arthroscopic results, the remaining 20 false positive cases seemed to be affected by the combined fluid collection in the long head of biceps tendon sheath or subcortical cysts in the lesser tuberosity.

Table 4. Interobserver Agreements of Three Readers in Evaluating Rotator Cuff Tears

		Reader 1-2 P-value	Reader 1-3 P-value	Reader 2-3 P-value
SST-IST tear				
FT+PT	3D TSE-SPACE	0.863 (-0.045, 0.054)	0.763 (-0.040, 0.054)	0.920 (-0.053, 0.059)
	2D TSE	0.544 (-0.036, 0.067)	0.784 (-0.027, 0.036).	0.675 (-0.043, 0.066)
PT	3D TSE-SPACE	0.583 (-0.068, 0.121)	0.472 (-0.056, 0.120)	0.920 (-0.109, 0.121)
	2D TSE	0.559 (-0.069, 0.128)	0.786 (-0.055, 0.072)	0.700 (-0.084, 0.125)
SCT tear				
	3D TSE-SPACE	0.454 (-0.066, 0.147)	0.007 (0.042, 0.258)	0.012 (0.024, 0.194)
	2D TSE	0.910 (-0.066, 0.074)	0.061 (-0.003, 0.136)	0.065 (-0.004, 0.145)

2D = two-dimensional; 3D TSE-SPACE = three-dimensional isotropic fat-suppressed turbo spin-echo SPACE intermediate-weighted image; FT = full-thickness tear; PT = partial-thickness tear; SCT = subscapularis tendon; SST-IST = supraspinatus and infraspinatus tendon

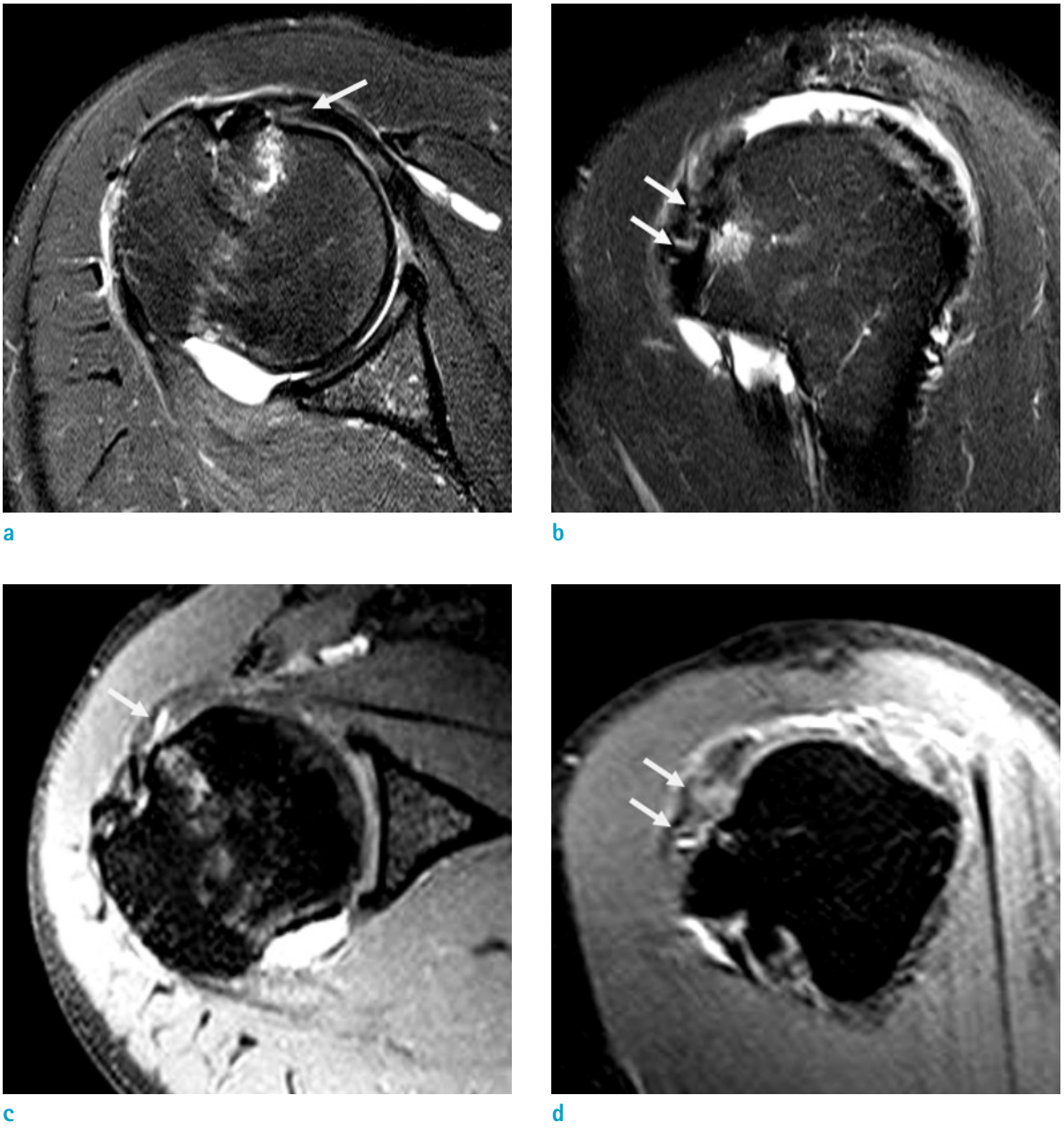

Fig. 4. Non-arthrographic MR images show arthroscopically-proven grade 2 partial-thickness articular-sided tear of the SCT in a 56-year-old woman. (a, b) Axial and oblique sagittal fat-suppressed T2-weighted images and (c, d) 3D isotropic fat-suppressed intermediate-weighted TSE-SPACE images with an axial and an oblique sagittal reformation show a high signal intensity area at the articular surface of SCT, which involves more than one third of the craniocaudal diameter of the tendon (arrows). A subcortical cyst is present in the lesser tuberosity of proximal humerus. All three readers correctly interpreted this case on both 2D sequences and TSE-SPACE.

DISCUSSION

The higher resolution with thinner slice thickness and shortened imaging time of 3T MRI enable us to obtain diagnosable MR images for rotator cuff tears without arthrography. The diagnostic performance of 3D isotropic sequences for detecting rotator cuff tears has been previously described on direct or indirect MR arthrography of shoulder at 3T system (5, 8-11, 19, 20). Regarding 3D isotropic FSE sequence in MR arthrography, previous studies

(5, 9-11) have reported the sensitivity and specificity for the detection of SST-IST tears to be between 89-97% and 77-93%, respectively. In our study, the mean sensitivity and specificity of TSE-SPACE were 95% and 100%, values consistent with those of previous studies (5, 9-11) and not significantly different from those of 2D sequences.

There have been reports (9-11, 19) assessing SCT tears on 3D isotropic sequence in direct and indirect MR arthrography. Two of them used FSE, one of them used the gradient-refocused echo technique, and the other used both. The previous studies (10, 11) using FSE 3D isotropic sequence in the diagnosis of SCT tears in direct MR arthrography reported mean sensitivities of 87% and 95%, respectively, and mean specificities of 90% and 65%, respectively. The other report (9) using the FSE technique on indirect MR arthrography reported a mean sensitivity of 81% and a mean specificity of 88%. Without intraarticular injection, our study revealed lower sensitivity and specificity (87% and 49%, respectively) for SCT tears than those of Choo et al. (11); however, our study showed a higher sensitivity and lower specificity than those of Lee et al. (9). Moreover, in our study, TSE-SPACE is shown to be less reliable than 2D sequences, as measured with the AUC, for detecting SCT tears in non-arthrographic MRI.

In our study, TSE-SPACE showed similar mean sensitivity, but lower mean specificity, compared to that of 2D sequences in the diagnosis of SCT tears, and also had more false positive cases. The low specificity of TSE-SPACE in our study was thought to be influenced by the blurring effect which accentuates the signal of joint fluid or concomitant pathology of the long head of biceps tendon or underlying bone. TSE-SPACE has more of a blurring effect due to the T2 decay, which reduces the amplitude of the high spatial frequency, during the long echo train (13, 21, 22). In addition, the longer imaging time of TSE-SPACE may induce more motion artifacts than 2D sequences. In our study, there were seven false positive cases of SCT tears, which were noted on both 2D sequences and TSE-SPACE in all three readers and still suspicious on the second review. As the tendon footprint is not well visualized with arthroscopy, mid to distal foot print tears can be missed (23, 24).

Magee and Williams (25) have found highly favorable sensitivity (98% for full-thickness tears and 92% for partial-thickness tears) and specificity (96% for full-thickness tears and 100% for partial-thickness tears) of 3T non-arthrographic MRI of shoulder in the diagnosis of SST tears. They included 98 full-thickness tears and 26 partial-thickness tears of SST. Meanwhile, 51% (34/69) of our study group had partial-thickness tears in all of the SST-IST tears. Our study revealed higher sensitivity (100% for full-thickness tears and 97% for partial-thickness tears) and lower specificity (93%) for SST-IST tears on 2D sequences. However, only five negative cases were included in our study, and the specificity of one reader was 80% by missing one case. The specificity of the other two readers was 100%. Thus, it would be hard to conclude that the specificity of our study is low.

Several studies (9-11, 19, 26-29) have reported the diagnostic performance of SCT tears on conventional 2D sequences. Gyftopoulos et al. (28) used both 1.5T and 3T non-arthrographic MRI for the evaluation of SCT tears in a retrospective study of 244 patients, of which 25 (10%) had tears. Without differentiating between 1.5T and 3T MRIs, the sensitivity, specificity, and accuracy were 80%, 91%, and 90%, respectively. The other reports (9-11, 19, 26, 27, 29) were all based on direct or indirect MR arthrography, and the sensitivity level ranged from 64 to 95% with the specificity level ranging from 57 to 100% in the detection of SCT tears. In our study, the mean sensitivity and specificity of the three readers on 2D sequences (88% and 66%, respectively) were in range of those in previous radiology reports.

There were several limitations in this study. First, this was a retrospective study. Therefore, selection bias existed. Second, there was a verification bias because arthroscopically-proven cases were included in this study; the radiologists who participated in the image analysis knew that the study group had undergone arthroscopy. Third, we used arthroscopy as a reference standard. However, arthroscopy is operator dependent and might exhibit interobserver variability, especially for the footprint tears of SCT. Fourth, since the 2D sequences were always acquired before the TSE-SPACE images, those images of TSE-SPACE were more influenced by patient motion. This could cause bias in the performance of TSE-SPACE. Fifth, all of the readers of this study were more familiar to arthrographic images and had short experience of non-arthrographic 3D isotropic sequence. With more experience of non-arthrographic MRI with evoluted 3D isotropic sequence, we might yield higher interobserver agreements and AUCs for the SCT tears on TSE-SPACE.

In conclusion, TSE-SPACE may have accuracy and reliability that are comparable to those of conventional 2D sequences for SST-IST tears on non-arthrographic 3T shoulder MRI, whereas TSE-SPACE is less reliable than conventional 2D sequences in detecting SCT tears.

Acknowledgments

This work is supported by Musculoskeletal MR Study Group, Korean Society of Magnetic Resonance in Medicine, 2017.

REFERENCES

1. de Jesus JO, Parker L, Frangos AJ, Nazarian LN. Accuracy of MRI, MR arthrography, and ultrasound in the diagnosis of rotator cuff tears: a meta-analysis. AJR Am J Roentgenol 2009;192:1701-1707
2. Shapiro L, Staroswiecki E, Gold G. Magnetic resonance imaging of the knee: optimizing 3 Tesla imaging. Semin Roentgenol 2010;45:238-249
3. Gold GE, Suh B, Sawyer-Glover A, Beaulieu C. Musculoskeletal MRI at 3.0 T: initial clinical experience. AJR Am J Roentgenol 2004;183:1479-1486
4. Steinbach LS, Palmer WE, Schweitzer ME. Special focus session. MR arthrography. Radiographics 2002;22:1223-1246
5. Jung JY, Jee WH, Park MY, Lee SY, Kim YS. Supraspinatus tendon tears at 3.0 T shoulder MR arthrography: diagnosis with 3D isotropic turbo spin-echo SPACE sequence versus 2D conventional sequences. Skeletal Radiol 2012;41:1401-1410
6. Jung JY, Jee WH, Park MY, Lee SY, Kim YS. SLAP tears: diagnosis using 3-T shoulder MR arthrography with the 3D isotropic turbo spin-echo space sequence versus conventional 2D sequences. Eur Radiol 2013;23:487-495
7. Jung JY, Yoon YC, Choi SH, Kwon JW, Yoo J, Choe BK. Three-dimensional isotropic shoulder MR arthrography: comparison with two-dimensional MR arthrography for the diagnosis of labral lesions at 3.0 T. Radiology 2009;250:498-505
8. Magee T. Can isotropic fast gradient echo imaging be substituted for conventional T1 weighted sequences in shoulder MR arthrography at 3 Tesla? J Magn Reson Imaging 2007;26:118-122
9. Lee JH, Yoon YC, Jee S, Kwon JW, Cha JG, Yoo JC. Comparison of three-dimensional isotropic and two-dimensional conventional indirect MR arthrography for the diagnosis of rotator cuff tears. Korean J Radiol 2014;15:771-780
10. Park SY, Lee IS, Park SK, Cheon SJ, Ahn JM, Song JW. Comparison of three-dimensional isotropic and conventional MR arthrography with respect to the diagnosis of rotator cuff and labral lesions: focus on isotropic fat-suppressed proton density and VIBE sequences. Clin Radiol 2014;69:e173-182
11. Choo HJ, Lee SJ, Kim OH, Seo SS, Kim JH. Comparison of three-dimensional isotropic T1-weighted fast spin-echo MR arthrography with two-dimensional MR arthrography of the shoulder. Radiology 2012;262:921-931
12. Kijowski R, Davis KW, Blankenbaker DG, Woods MA, Del Rio AM, De Smet AA. Evaluation of the menisci of the knee joint using three-dimensional isotropic resolution fast spin-echo imaging: diagnostic performance in 250 patients with surgical correlation. Skeletal Radiol 2012;41:169-178
13. Kijowski R, Davis KW, Woods MA, et al. Knee joint: comprehensive assessment with 3D isotropic resolution fast spin-echo MR imaging--diagnostic performance compared with that of conventional MR imaging at 3.0 T. Radiology 2009;252:486-495
14. Notohamiprodjo M, Horng A, Pietschmann MF, et al. MRI of the knee at 3T: first clinical results with an isotropic PDfs-weighted 3D-TSE-sequence. Invest Radiol 2009;44:585-597
15. Notohamiprodjo M, Kuschel B, Horng A, et al. 3D-MRI of the ankle with optimized 3D-SPACE. Invest Radiol 2012;47:231-239
16. Ristow O, Steinbach L, Sabo G, et al. Isotropic 3D fast spin-echo imaging versus standard 2D imaging at 3.0 T of the knee--image quality and diagnostic performance. Eur Radiol 2009;19:1263-1272
17. Yao L, Pitts JT, Thomasson D. Isotropic 3D fast spin-echo with proton-density-like contrast: a comprehensive approach to musculoskeletal MRI. AJR Am J Roentgenol 2007;188:W199-201
18. Altman DG. Practical statistics for medical research. London: Chapman & Hall, 1991:404-409
19. Oh DK, Yoon YC, Kwon JW, et al. Comparison of indirect isotropic MR arthrography and conventional MR arthrography of labral lesions and rotator cuff tears: a prospective study. AJR Am J Roentgenol 2009;192:473-479
20. Park HJ, Lee SY, Kim MS, et al. Evaluation of shoulder pathology: three-dimensional enhanced T1 high-resolution isotropic volume excitation MR vs two-dimensional fast spin echo T2 fat saturation MR. Br J Radiol 2015;88:20140147
21. Stevens KJ, Busse RF, Han E, et al. Ankle: isotropic MR imaging with 3D-FSE-cube--initial experience in healthy volunteers. Radiology 2008;249:1026-1033
22. Van Dyck P, Gielen JL, Vanhoenacker FM, et al. Diagnostic performance of 3D SPACE for comprehensive knee joint assessment at 3 T. Insights Imaging 2012;3:603-610
23. Koo SS, Burkhart SS. Subscapularis tendon tears: identifying mid to distal footprint disruptions. Arthroscopy 2010;26:1130-1134
24. David TS, Bravo H, Scobercea R. Arthroscopic visualization

of subscapularis tendon lesions. Orthopedics 2009;32
25. Magee T, Williams D. 3.0-T MRI of the supraspinatus tendon. AJR Am J Roentgenol 2006;187:881-886
26. Jung JY, Yoon YC, Yi SK, Yoo J, Choe BK. Comparison study of indirect MR arthrography and direct MR arthrography of the shoulder. Skeletal Radiol 2009;38:659-667
27. Pfirrmann CW, Zanetti M, Weishaupt D, Gerber C, Hodler J. Subscapularis tendon tears: detection and grading at MR arthrography. Radiology 1999;213:709-714
28. Gyftopoulos S, O' Donnell J, Shah NP, Goss J, Babb J, Recht MP. Correlation of MRI with arthroscopy for the evaluation of the subscapularis tendon: a musculoskeletal division's experience. Skeletal Radiol 2013;42:1269-1275
29. Jung JY, Jee WH, Chun CW, Kim YS. Diagnostic performance of MR arthrography with anterior trans-subscapularis versus posterior injection approach for subscapularis tendon tears at 3.0T. Eur Radiol 2017;27:1303-1311